Proceedings of OMAE03
22nd International Conference on Offshore Mechanics and Arctic Engineering
June 8–13, 2003, Cancun, Mexico

OMAE2003-37087

MULTI-LAYER MODELING OF WAVE GROUPS FROM DEEP TO SHALLOW WATER

Patrick Lynett *
Ocean and Coastal Division
Department of Civil Engineering
Texas A&M University
College Station, TX 77843
Email: plynett@civil.tamu.edu

Philip L.-F. Liu
School of Civil and Environmental Engineering
Cornell University
Ithaca, NY 14850
Email: pll3@cornell.edu

Hwung-Hweng Hwung
Wen-Son Ching
Tainan Hydraulics Laboratory
Hydraulics & Ocean Engineering Department
National Cheng Kung University
Taiwan

ABSTRACT

A set of model equations for water wave propagation is derived by piecewise integration of the primitive equations of motion through N arbitrary layers. Within each layer, an independent velocity profile is determined. With N separate velocity profiles, matched at the interfaces of the layers, the resulting set of equations have N+1 free parameters, allowing for an optimization with known analytical properties of water waves. The optimized two-layer model equations show good linear wave characteristics up to $kh \approx 8$, while the second-order nonlinear behavior is well captured to $kh \approx 6$. The three-layer model shows good linear accuracy to $kh \approx 14$, and the four layer to $kh \approx 20$. A numerical algorithm for solving the model equations is developed and tested against nonlinear deep-water wave-group experiments, where the kh of the carrier wave in deep water is around 6. The experiments are set up such that the wave groups, initially in deep water, propagate up a constant slope until reaching shallow water. The overall comparison between the multi-layer model and the experiment is quite good, indicating that the multi-layer theory has good nonlinear, as well has linear, accuracy for deep-water waves.

Introduction

The past decade saw the advent and wide spread applications of Boussinesq-type equation models for studying water wave propagation in one and two horizontal dimensions. This depth-integrated modeling approach employs a polynomial approximation of the vertical profile of the velocity field, thereby reducing the dimensions of a three dimensional problem by one. The conventional Boussinesq equations (Peregrine, 1967) and the generalized Boussinesq equations of Wu (1981), which make use of a quadratic polynomial approximation for the vertical flow distribution, have two major constraints: (1) The depth-averaged model poorly describes the frequency dispersion of wave propagation in intermediate depths, and (2) the weakly nonlinear assumption limits the largest wave height that can accurately be modeled. These constraints are consistent with the fundamental assumption of the Boussinesq equations, which states that leading order dispersion and nonlinear effects are of the same order and are weak, i.e., $O(\mu_o^2) = O(\varepsilon_o) \ll 1$, where μ_o = wavenumber times depth (kh) and ε_o = amplitude over depth (a/h). The dispersive properties of the conventional Boussinesq equations have been improved by modifying the dispersive terms (Madsen & Sorensen, 1992) or using a reference velocity at a specified depth (Nwogu, 1993). These techniques yield a set of equations whose linear dispersion relation can be adjusted such that the resulting intermediate-depth dispersion characteristics are close to those of linear wave theory. Liu (1994) and Wei *et al.* (1995) extended Nwogu's approach to highly nonlinear waves, developing models that not only can be applied to intermediate water depth but also are capable of simulating wave propagation with strong nonlinear interaction, i.e. $\varepsilon_o = O(1)$. In general, these model equations contain accurate linear dispersion properties to $kh \approx 3$ (e.g. Nwogu, 1993). In intermediate depths, nonlinear properties tend to exhibit larger relative errors than linear properties (Madsen & Schäffer, 1998), although additional enhancements

*Address all correspondence to this author.

can indeed create accurate nonlinear characteristics to near the linear accuracy limit, $kh \approx 3$ (Kennedy *et al.*, 2001).

Further enhancing the deep water accuracy of the depth-integrated approach is the so-called high-order Boussinesq-type equations. While the model equations described in the previous paragraph use a quadratic polynomial approximation for the vertical flow distribution, these high-order models use fourth, and higher, order polynomial approximations. Gobbi *et al.* (2000), using a fourth-order polynomial, developed a model with excellent linear dispersive properties up to $kh \approx 6$. Nonlinear behavior was faithfully captured to $kh \approx 3$. With the drastic improvement in accuracy over previous model equations comes a significant computational increase as well. The fourth-order polynomial employed results in fifth-order spatial derivatives in an extremely complex equation system, requiring an equally complex numerical scheme. Madsen & Schäffer (1998) and Agnon *et al.* (1999) derived model equations with even higher order polynomial approximations. The highest order of spatial differentiation in these model equations increases linearly with the order of polynomial approximation. Additionally, the complexity increases again for a two-horizontal dimension (2HD) problem, for which no high-order modeling attempts have yet been made. The reader is directed to Madsen & Schäffer (1998), a thorough analysis of numerous different depth-integrated model equations, for additional information.

In this paper, a different approach to obtaining a high-order, depth-integrated model is taken. Instead of employing a high-order polynomial approximation for the vertical distribution of the flow field, N quadratic polynomials are used, matched at an interface that divides the water column into N layers. This approach leads to a set of model equations without the high-order spatial derivatives associated with high-order polynomial approximations. The multi-layer concept has been attempted previously by Kanayama *et al.* (1998), although the derivation and final model equations are quite different from those to be presented here. Internal wave and stratified flow modelers often employ a multi-layering concept, although the layers are always layers of different density and thus represent a very dissimilar physical problem than the one examined in this paper. Madsen *et al.* (2002) developed a model, based on the method of Agnon *et al.* (1999), accurate to extremely deep water ($kh \approx 40$). Their derivation, fundamentally different from the one presented in this paper, involves optimal expansions of the Laplace equation, allowing for excellent deep water linear and nonlinear dispersive properties of the resulting model. By using multiple expansions at various levels in the water column, the deep water accuracy is achieved while only requiring the fifth-order spatial derivatives found in alternative high-order models with much smaller deep water limitations. However, Madsen *et al.*'s model consists of more equations than the alternative models, and thus more unknowns. This is quite similar to the basic idea of the multi-layer derivation presented here: to trade fewer unknowns and higher spatial derivatives for more unknowns and lower spatial derivatives.

In the first section of this paper, the derivation of the N-layer, depth-integrated model is presented. Analysis of the model follows, including examination of linear dispersion, shoaling, and nonlinear properties. These properties are optimized, based on agreements with linear and Stokes wave theories, and it is shown that the N-layer model is accurate into deep water. Finally, a numerical algorithm is developed for the general 2HD problem, and numerical solutions are compared with experimental data for deep water wave propagation. The N-layer equation system exhibits significant improvement over previous models.

1 Governing Equations & Boundary Conditions

The goal of this derivation is to formulate a set of equations by integrating the primitive equations of motion. The integration will be performed piecewisely. As shown in Figure 1, $\zeta'(x',\, y',\, t')$ denotes the free surface displacement of a wave train propagating in the water depth $h'(x',\, y',\, t')$. The boundary between layers are given as $\eta'_n(x',\, y',\, t')$. The system will be divided into N layers, where the upper and lower boundaries are given by $\eta'_o = \zeta'$ and $\eta'_N = -h'$, respectively. All of the other boundaries will be constructed as $\eta'_n = \alpha_n h' + \beta_n \zeta'$, where α_n and β_n are arbitrary and user defined. Note that both h' and ζ' are functions of time, and therefore so is η'_n. Each of the N layers has a characteristic thickness, d_n, as defined by Figure 1. Utilizing the layer thicknesses d_n as the vertical length scales in the corresponding layers, h_o as the characteristic water depth, the characteristic length of the wave ℓ_o=$1/k$ as the horizontal length scale, $\ell_o/\sqrt{gh_o}$ as the time scale, and the characteristic wave amplitude a_o as the scale of wave motion, we can define the following dimensionless variables:

$$(x,\, y) = (x',\, y')/\ell_o,\;\; z_n = z'/d_n,\;\; t = \sqrt{gh_o}\,t'/\ell_o,\;\; p_n = p'_n/\rho g a_o$$

$$h = h'/h_o,\;\; \zeta = \zeta'/a_o,\;\; \eta_n = \eta'_n/b_n$$

$$(U_n,\, V_n) = (U'_n,\, V'_n)/\left(\varepsilon_o\sqrt{gh_o}\right),\;\; W_n = W'_n/\left[\varepsilon_o\mu_o\sqrt{gh_o}\right] \quad (1)$$

in which the subscript n indicates the layer index, $b_o = a_o$, $b_n = \sum_{m=1}^{n} d_m$ for $n = 1$ to N, (U_n, V_n) represent the horizontal velocity components in the different layers, W_n the vertical velocity component in the layers, and p_n the pressures. Note that the subscript on z indicates that the vertical coordinate is scaled

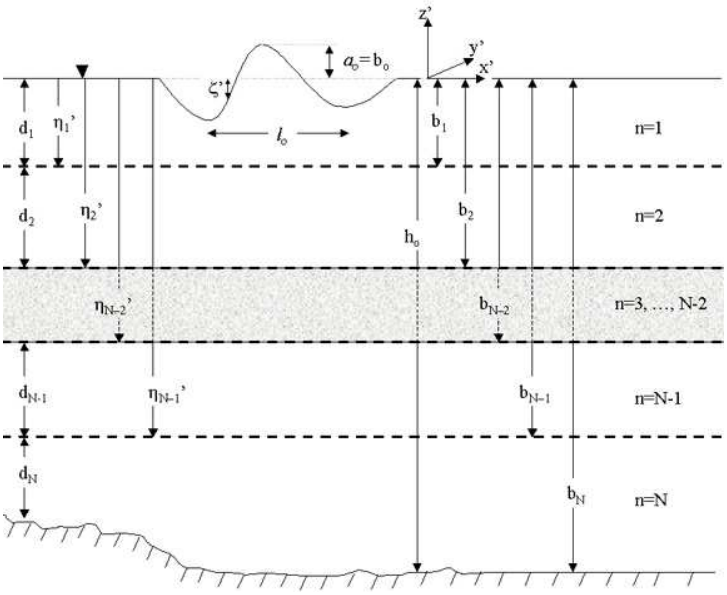

Figure 1. N-Layer problem setup.

differently in each layer. Dimensionless parameters have been introduced in (1), which are

$$\varepsilon_o = a_o/h_o, \;\; \mu_o = h_o/\ell_o \tag{2}$$

It is reiterated that $\ell_o = 1/k$, and thus μ_o=kh_o. Assuming that the viscous effects are insignificant, the wave motion can be described by the continuity equation and the Euler's equations, i.e.,

$$\frac{d_n}{h_o}\nabla\cdot U_n + \frac{\partial W_n}{\partial z_n} = 0 \tag{3}$$

$$\frac{\partial U_n}{\partial t} + \varepsilon_o U_n\cdot\nabla U_n + \varepsilon_n W_n\frac{\partial U_n}{\partial z_n} = -\nabla p_n \tag{4}$$

$$\mu_n^2\left(\frac{\partial W_n}{\partial t} + \varepsilon_o U_n\cdot\nabla W_n\right) + \varepsilon_o\mu_o^2 W_n\frac{\partial W_n}{\partial z_n} = -\left(\frac{\partial p_n}{\partial z_n} + \frac{1}{\varepsilon_n}\right) \tag{5}$$

where $\mu_n = d_n h_o/l_o^2$, $\varepsilon_n = a_o/d_n$, $U_n = (U_n, V_n)$ denotes the horizontal velocity vector, and $\nabla = (\partial/\partial x,\ \partial/\partial y)$ the horizontal gradient vector.

On the free surface, $z_1 = \varepsilon_1\zeta(x,\, y,\, t)$ the usual kinematic and dynamic boundary condition applies:

$$W_1 = \frac{\partial\zeta}{\partial t} + \varepsilon_o U_1\cdot\nabla\zeta \;\; \text{on } z_1 = \varepsilon_1\zeta \tag{6}$$

$$p_1 = 0 \;\; \text{on } z_1 = \varepsilon_1\zeta \tag{7}$$

Along the seafloor, $z_N = -\frac{h_o}{d_N}h$, the kinematic boundary condition requires

$$W_N + U_N\cdot\nabla h + \frac{1}{\varepsilon_o}\frac{\partial h}{\partial t} = 0, \;\; \text{on } z_N = -\frac{h_o}{d_N}h \tag{8}$$

At the imaginary interface between the layers, continuity of pressure and velocity is required:

$$p_n = p_{n+1}, \;\; \text{on } z_n = \frac{b_n}{d_n}\eta_n,\ z_{n+1} = \frac{b_n}{d_{n+1}}\eta_n \;\; \text{for } n = 1, N-1 \tag{9}$$

$$U_n = U_{n+1}, \;\; \text{on } z_n = \frac{b_n}{d_n}\eta_n,\ z_{n+1} = \frac{b_n}{d_{n+1}}\eta_n \;\; \text{for } n = 1, N-1 \tag{10}$$

$$W_n = W_{n+1}, \;\; \text{on } z_n = \frac{b_n}{d_n}\eta_n,\ z_{n+1} = \frac{b_n}{d_{n+1}}\eta_n \;\; \text{for } n = 1, N-1 \tag{11}$$

For later use, we note here that the depth-integrated continuity equation can be obtained by integrating (3) across each of the layers. After applying the boundary conditions (10), (11), (6), and (8), the resulting equation reads

$$\nabla\cdot\left[\sum_{n=1}^{N}\frac{d_n}{h_o}\int_{\frac{b_n}{d_n}\eta_n}^{\frac{b_{n-1}}{d_n}\eta_{n-1}} U_n dz\right] + \frac{1}{\varepsilon_o}\frac{\partial h}{\partial t} + \frac{\partial\zeta}{\partial t} = 0 \tag{12}$$

We remark here that (12) is exact.

2 Approximate 2-HD Governing Equations

A perturbation analysis will be performed utilizing the assumption

$$O(\mu_n^2) \ll 1. \tag{13}$$

Using μ_n^2 as the small parameter, we can expand the dimensionless physical variables as power series of μ_n^2

$$f = \sum_{M=0}^{\infty}\mu_n^{2M} f^{[M]}; \;\; (f = U_n, W_n, \zeta, p_n) \tag{14}$$

Furthermore, we will adopt the irrotationality assumption on the vorticity field. With the above assumptions, the vertical profile of vertical velocity is given as:

$$W_n = -z_n S_n - T_n + O(\mu_n^2) \tag{15}$$

where

$$S_n = \frac{d_n}{h_o}\nabla\cdot U_n$$

$$T_n = \sum_{m=n}^{N-1}\eta_m\left(\frac{b_m}{d_{m+1}}S_{m+1} - \frac{b_m}{d_m}S_m\right) + \nabla\cdot(hU_N) + \frac{1}{\varepsilon_o}\frac{\partial h}{\partial t} \quad (16)$$

and the horizontal velocity is expressed by:

$$U_n = u_n - \mu_n^2\left\{\frac{z^2-\kappa_n^2}{2}\nabla S_n + (z-\kappa_n)\nabla T_n\right\} + O(\mu_n^4) \quad (17)$$

where $u_n(x,\ y,\ \kappa_n(x,\ y,\ t),\ t)$ is the horizontal velocity evaluated at $z = \kappa_n(x,\ y,\ t)$.

The exact continuity equation (12) can be rewritten approximately in terms of ζ and u_n. Substituting (17) into (12), we obtain

$$\frac{1}{\varepsilon_o}\frac{\partial h}{\partial t} + \frac{\partial\zeta}{\partial t} + \nabla\cdot\sum_{n=1}^{N}\left(\frac{b_{n-1}}{h_o}\eta_{n-1} - \frac{b_n}{h_o}\eta_n\right)u_n - \nabla\cdot\sum_{n=1}^{N}\mu_n^2\frac{d_n}{h_o}$$

$$\left\{\left[\frac{\left(\frac{b_{n-1}}{d_n}\eta_{n-1}\right)^3 - \left(\frac{b_n}{d_n}\eta_n\right)^3}{6} - \frac{(\frac{b_{n-1}}{d_n}\eta_{n-1} - \frac{b_n}{d_n}\eta_n)z_n^2}{2}\right]\nabla S_n\right.$$

$$\left. + \left[\frac{\left(\frac{b_{n-1}}{d_n}\eta_{n-1}\right)^2 - \left(\frac{b_n}{d_n}\eta_n\right)^2}{2} - (\frac{b_{n-1}}{d_n}\eta_{n-1} - \frac{b_n}{d_n}\eta_n)z_n\right]\nabla T_n\right\}$$

$$= O(\mu_n^4) \quad (18)$$

Equation (18) is one of three governing equations for ζ and u_n. One of the remaining equations comes from the horizontal momentum equation, (4). To derive the governing equations for u_1, we first substitute (17) and the pressure expression (not shown here) into (4) yields the following equation,

$$\frac{\partial u_1}{\partial t} + \varepsilon_o u_1\cdot\nabla u_1 + \nabla\zeta + \mu_1^2\frac{\partial}{\partial t}\left\{\frac{\kappa_1^2}{2}\nabla S_1 + \kappa_1\nabla T_1\right\}$$

$$+\varepsilon_o\mu_1^2[(u_1\cdot\nabla\kappa_1)\nabla T_1 + \kappa_1\nabla(u_1\cdot\nabla T_1) + \kappa_1(u_1\cdot\nabla\kappa_1)\nabla S_1 +$$

$$\frac{\kappa_1^2}{2}\nabla(u_1\cdot\nabla S_1)] + \varepsilon_o\mu_o^2\left[T_1\nabla T_1 - \nabla\left(\zeta\frac{\partial T_1}{\partial t}\right)\right]$$

$$+\varepsilon_o^2\mu_o^2\nabla\left(\zeta S_1 T_1 - \frac{h_o}{d_1}\frac{\zeta^2}{2}\frac{\partial S_1}{\partial t} - \zeta u_1\cdot\nabla T_1\right)$$

$$+\varepsilon_o^2\varepsilon_1\mu_o^2\nabla\left[\frac{\zeta^2}{2}\left(S_1^2 - \frac{h_o}{d_1}u_1\cdot\nabla S_1\right)\right] = O\left(\mu_o^2\mu_1^2\right) \quad (19)$$

It is remarked here that $\varepsilon_o\mu_o^2 = \varepsilon_1\mu_1^2$, and all coefficients are written in terms of μ_o and ε_o whenever possible. Determination of u_n for $n = 2, N$ does not require solving additional momentum equations. With boundary condition (10) and the known velocity profiles (17), u_n can be explicitly given as a function of u_{n-1}:

$$u_n + \mu_n^2\left\{\frac{\kappa_n^2 - \left(\frac{b_{n-1}}{d_n}\eta_{n-1}\right)^2}{2}\nabla S_n + \left(\kappa_n - \frac{b_{n-1}}{d_n}\eta_{n-1}\right)\nabla T_n\right\} =$$

$$u_{n-1} + \mu_{n-1}^2\left\{\frac{\kappa_{n-1}^2 - \left(\frac{b_{n-1}}{d_{n-1}}\eta_{n-1}\right)^2}{2}\nabla S_{n-1} +\right.$$

$$\left.\left(\kappa_{n-1} - \frac{b_{n-1}}{d_{n-1}}\eta_{n-1}\right)\nabla T_{n-1}\right\} + O(\mu_{n-1}^4, \mu_n^4) \quad (20)$$

Thus, the lower layer velocities can be directly calculated with knowledge of the upper layer velocity. Equations (18), (19), and (20) are the coupled governing equations, written in terms of u_n and ζ, for highly nonlinear, dispersive waves.

A question that arises with the use of the matched velocity profiles in each layer is whether the vertical velocity gradients are continuous across the layer boundary, which is not a directly enforced boundary condition. If the gradients are not continuous, there is a discontinuity of the nonlinear, vertical transport terms in the horizontal and vertical Euler's equations. Specifically, the discontinuity would arise in the $W_n(\partial U_n/\partial z_n)$ term in (4) and the

$\mu_o^2 W_n(\partial W_n/\partial z_n)$ term in (5). However, with calculation of these nonlinear terms using the derived vertical velocity profiles, (15), and horizontal velocity profiles, (17), it can readily be shown that the discontinuity is of the truncation error order in the final model, i.e.

$$\frac{\partial U_n(z_n=\frac{b_n}{d_n}\eta_n)}{\partial z_n} = \frac{\partial U_{n+1}(z_{n+1}=\frac{b_n}{d_{n+1}}\eta_n)}{\partial z_{n+1}} + O(\mu_n^4, \mu_{n+1}^4) \quad (21)$$

$$\mu_o^2 \frac{\partial W_n(z_n=\frac{b_n}{d_n}\eta_n)}{\partial z_n} = \mu_o^2 \frac{\partial W_{n+1}(z_{n+1}=\frac{b_n}{d_{n+1}}\eta_n)}{\partial z_{n+1}} + O(\mu_o^2\mu_n^2, \mu_o^2\mu_{n+1}^2) \quad (22)$$

Thus, the discontinuity of the nonlinear, vertical transport terms will not effect the overall accuracy of the model.

3 Accuracy of Multi-Layer Model

Through linear and nonlinear optimization of the interface and velocity evaluation locations (see Lynett & Liu, 2003; Lynett 2002), it is shown that the two-layer model exhibits accurate linear characteristics up to a $kh \approx 8$ and nonlinear accuracy to $kh \approx 6$. This is a greater than two-fold extension to higher kh over existing $O(\mu_o^2)$ Boussinesq-type models, while maintaining the maximum order of differentiation at three. A less thorough optimization of the three- and four-layer models is undertaken, examining only phase and group velocity. This optimization indicates that the three-layer model equations are accurate to $kh \approx 15$ and the four layer-model to $kh \approx 25$. Figure 2 summarizes the results from this chapter. This figure gives the phase and group velocity for the two-, three-, and four-layer models, as well as the traditional and high-order Boussinesq models.

4 Numerical Solutions

The numerical model employed here is identical to that described in Lynett & Liu (2003), which has its foundations in the high-order model presented by Wei & Kirby (1995). The numerical time-marching scheme is a fourth-order, implicit predictor-corrector method. The spatial derivatives are finite differenced to fourth-order accuracy. No filtering or other artificial numerical dissipation is utilized. As the equation form of the presented two-layer model is identical to the $O(\mu_o^2)$ Boussinesq-type equations, the numerical details, such as convergence criteria, are identical to those given in Wei *et al.* (1995) and Lynett & Liu (2002). For all of the numerical simulations presented in this paper, the lateral boundaries are modeled as absorbing boundaries through the use of sponge layers. The sponge layers are applied for both the one- and two-layer models as recommended by Kirby *et al.* (1998), which is an approach founded on the method presented by Israeli & Orszag (1981).

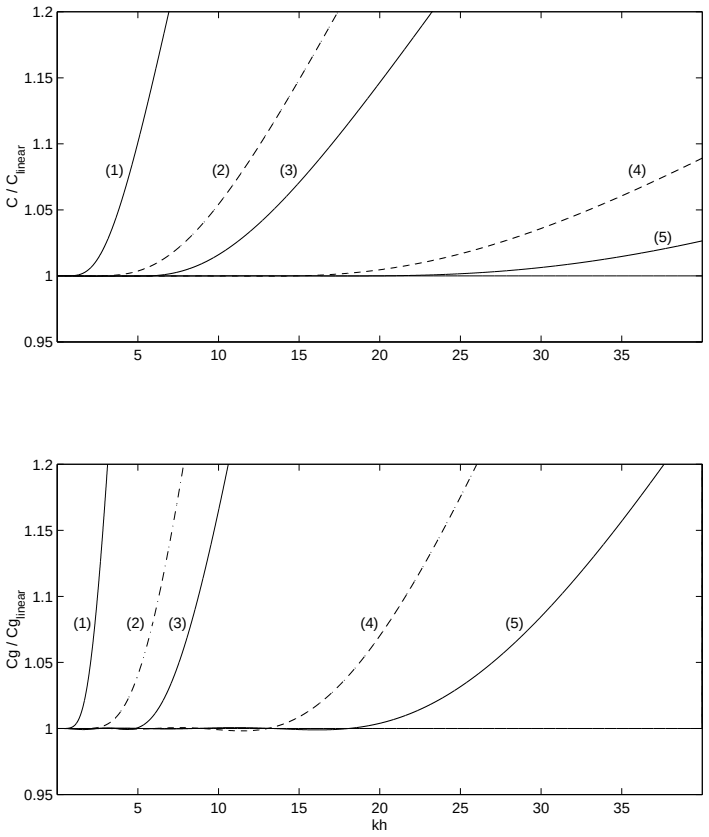

Figure 2. Comparison of wave speed and group velocity for numerous different models. Curve (1) is the [2,2] Pade properties used by some Boussinesq models, (2) is the [4,4] Pade of the high-order Boussinesq model, (3) is the two-layer model, (4) is the three-layer model, and (5) is the four-layer model.

5 Experimental Setup

The preliminary experiments were conducted in Hydraulic Laboratory of National Cheng-Kung University of Taiwan. Figure 3 shows the schematic diagram of the setup used in this study. The wave flume is approximately 300 m long, 5m wide and 5 m deep, and the experiments were conducted with a water depth of 3.5m. The arrangement of 39 wave-gauges is shown in Fig. 3. The waves were generated with a piston-type wave maker. The input signal consists of two wave components, linearly superimposed, with periods of 1.45 and 1.75 seconds. Each of the two components has an amplitude of 0.06 *m*.

6 Numerical Comparisons with Experimental Data

Figures 4 and 5 show the numerical results plotted with the experimental data for four locations along the tank. In Fig. 4 are two locations nearer to the wavemaker, at distances of 15 and 55*m* from the left boundary. Note that the wavelength of the car-

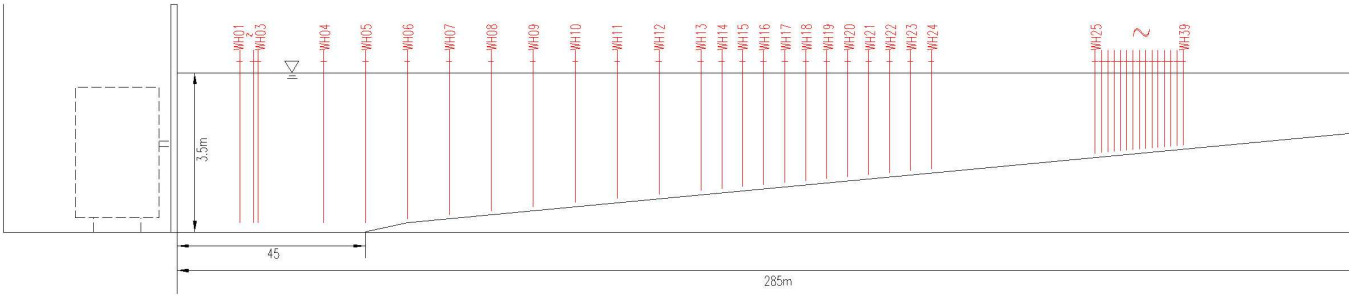

Figure 3. Experimental wave flume setup.

rier wave is on average 4 *m* over this range. As can be seen, the preliminary data is somewhat noisy, but overall, the agreement between the experimental data and the numerics is quite good. The numerical simulation appears to miss the high crests nearest to the wavemaker, although the agreement increases as the wave train moves further away from the generation region. Looking to Fig. 5, the numerical model is still in very good agreement at a distance of 115*m* from the wavemaker. It is not until much further downstream, at a distance of 195*m*, the differences between the numerical and experimental data are apparent. A phase shift is evident, with the numerical model predicting a faster phase velocity. This comparison occurs at a distance of nearly 50 wavelengths from the wavemaker, and accumulating numerical error may be the culprit.

7 Conclusions

A model for the transformation of highly nonlinear and dispersive waves is derived. The model utilizes N quadratic polynomials to approximate the vertical flow field, matched along an interface. Through linear and nonlinear optimization of the interface and velocity evaluation locations, it is shown that the two-layer model exhibits accurate linear characteristics up to a $kh \approx 8$ and nonlinear accuracy to $kh \approx 6$. This is a greater than two-fold extension to higher kh over existing $O(\mu_o^2)$ Boussinesq-type models, while maintaining the maximum order of differentiation at three. Owing to this maximum order of differentiation, a tractable numerical algorithm can be developed for the general 2HD problem, employing a well-studied predictor-corrector scheme. A set of preliminary wave group experiments have been performed at the National Cheng-Kung University of Taiwan and are presented here. Through the comparison with deep water wave group evolution, for which deep water nonlinear behavior is important, the multi-layer model is shown to be highly accurate. Some discrepancy between the experiment and numerics is found a fair distance from the wavemaker, and the experiments are currently being re-done in order to record a cleaner, more precise dataset.

ACKNOWLEDGMENT

The research reported here is partially supported by Grants from National Science Foundation (CMS-9528013, CTS-9808542, and CMS 9908392). We would also like to acknowledge the grant to National Cheng-Kung University from the Ministry of Education of Taiwan under the Program for Promoting University Academic Excellence (A-91-E-FA09-7-3).

REFERENCES

[1] AGNON, Y., MADSEN, P. A., AND SCHAFFER, H. 1999 A new approach to high order Boussinesq models. *J. Fluid Mech.* **399**, 319-333.

[2] GOBBI, M. F., KIRBY, J. T., AND WEI, G. 2000 A fully nonlinear Boussinesq model for surface waves. Part II. Extension to $O(kh)^4$. *J. Fluid Mech.* **405**, 182-210.

[3] KANAYAMA, S., TANAKA, H., AND SHUTO, N. 1998 A multi-level model for nonlinear dispersive water waves. In *Coastal Engineering 1998* (ed. Billy L. Edge), vol. 1, pp.576-588. ASCE.

[4] KENNEDY, A. B., KIRBY, J. T., CHEN, Q. AND DALRYMPLE, R. A. 2001 Boussinesq-type equations with improved nonlinear behaviour. *Wave Motion* **33**, 225-243.

[5] LIU, P. L.-F. 1994 Model equations for wave propagation from deep to shallow water. In *Advances in Coastal Engineering* (ed. P. L.-F. Liu), vol. 1, pp.125-157. World Scientific.

[6] LYNETT, P. 2002 A multi-layer approach to modeling nonlinear, dispersive waves from deep water to the shore. PhD thesis, Cornell University.

[7] LYNETT, P. AND LIU, P. L.-F. 2003 A multi-layer approach to wave modeling. *Journal of Fluid Mechanics* submitted.

[8] MADSEN, P. A., AND SORENSEN, O. R. 1992 A new form of the Boussinesq equations with improved linear dispersion characteristics. Part II: A slowly varying bathymetry. *Coast. Engng.* **18**, 183-204.

[9] MADSEN, P. A., AND SCHAFFER, H. A. 1998 Higher order Boussinesq-type equations for surface gravity waves - Derivation and analysis. *Royal Society of London A* **356**, 1-60.

[10] NWOGU, O. 1993 Alternative form of Boussinesq equa-

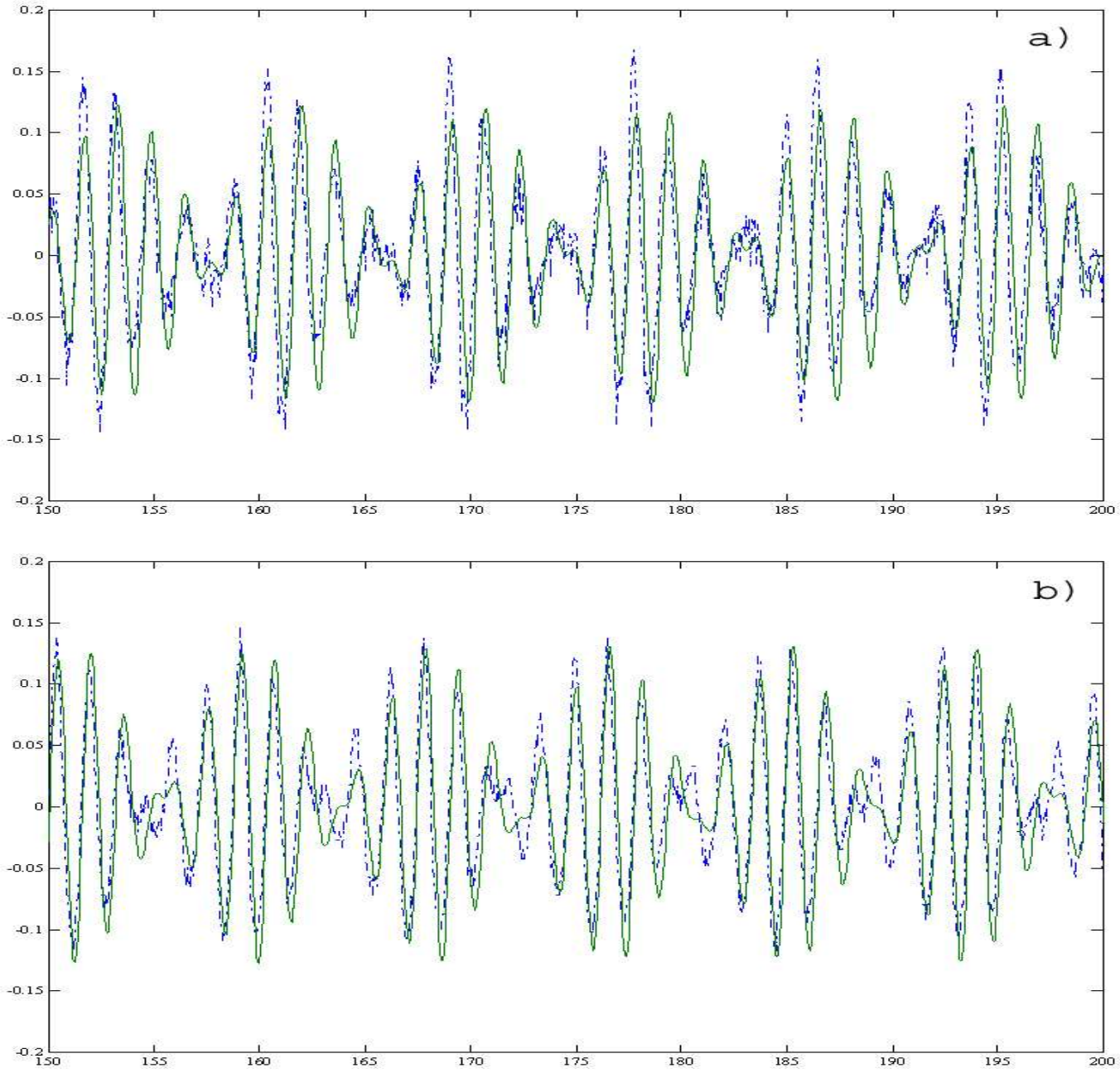

Figure 4. Experimental/numerical comparisons at distances from the wavemkaer of a)15m and b)55m. The solid line represents the numerical results and the dashed line the experimental data.

tions for nearshore wave propagation. *Journal of Waterway, Port, Coastal and Ocean Engng.* **119(6)**, 618-638.

[11] PEREGRINE, D. H. 1967 Long waves on a beach. *J. Fluid Mech.* **27**, 815-827.

[12] WEI, G. AND KIRBY, J. T. 1995 A time-dependent numerical code for extended Boussinesq equations. *Journal of Waterway, Port, Coastal and Ocean Engng.* **120**, 251-261.

[13] WEI, G., KIRBY, J. T., GRILLI, S. T., AND SUBRAMANYA, R. 1995 A fully nonlinear Boussinesq model for surface waves. Part I. Highly nonlinear unsteady waves. *J. Fluid Mech.* **294**, 71-92.

[14] WU, T. Y. 1981 Long waves in ocean and coastal waters.

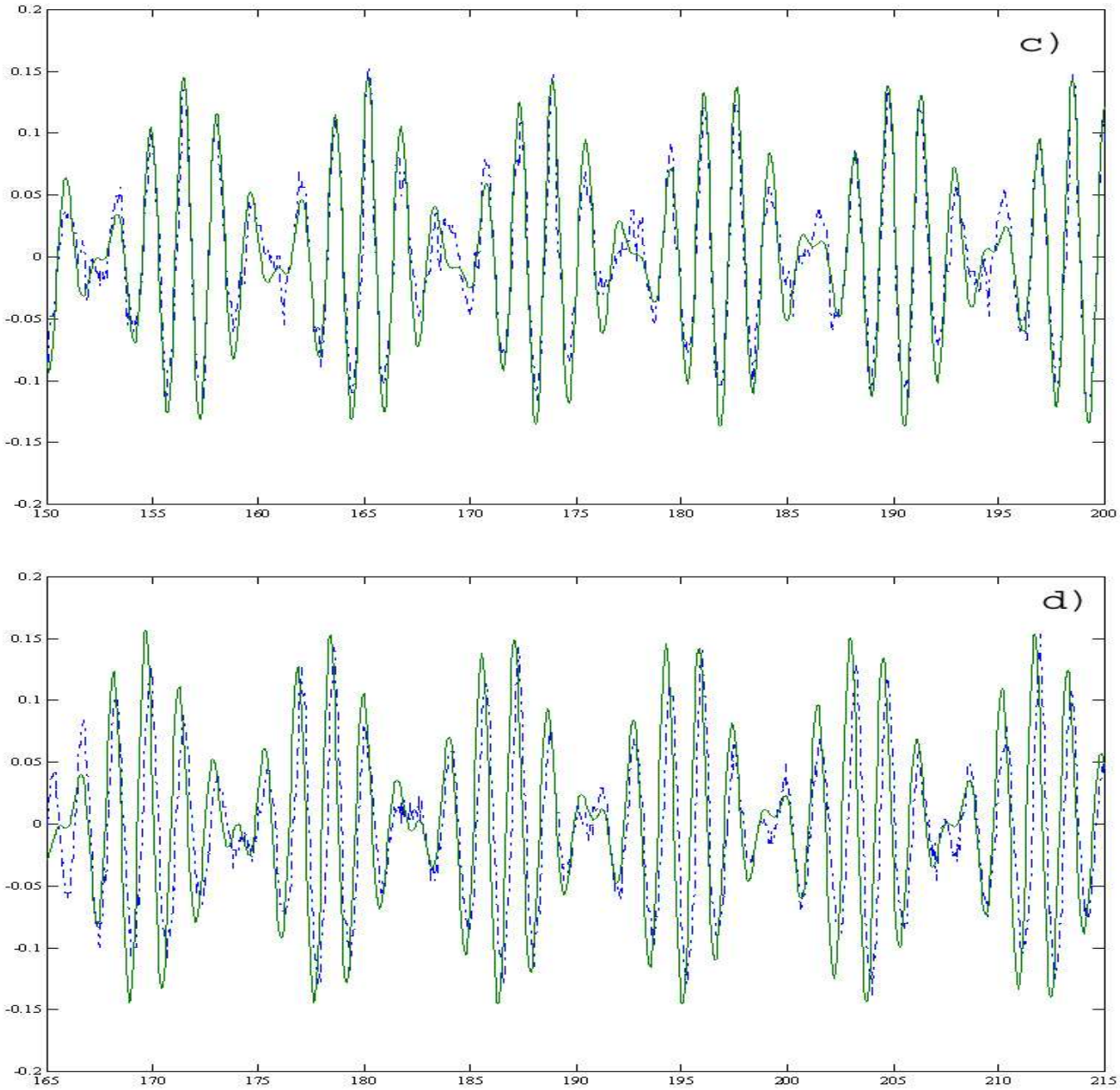

Figure 5. Experimental/numerical comparisons at distances from the wavemkaer of c)115m and d)195m. The solid line represents the numerical results and the dashed line the experimental data.

J. Engng. Mech. Div. ASCE **107**, 501-522.